Analytica Chimica Acta xxx (2018) 1–8

Contents lists available at ScienceDirect

Analytica Chimica Acta

journal homepage: www.elsevier.com/locate/aca

Integrated multichannel all-fiber optofluidic biosensing platform for sensitive and simultaneous detection of trace analytes

Wei Li [a, 1], Haoyu Wang [a, 1], Rong Yang [a], Dan Song [a], Feng Long [a, *], Anna Zhu [b, c, **]

[a] School of Environment and Natural Resources, Renmin University of China, Beijing, 100872, China
[b] Research Institute of Chemical Defense, Academy of Military Sciences PLA China, Beijing, 102205, China
[c] State Key Laboratory of NBC Protection FOR Civilian, Beijing, 102205, China

HIGHLIGHTS

- Integrated M-AOB was built for simultaneous detection of multiple trace analytes.
- Three SMFCs was used for transmission of excitation light and fluorescence.
- One detector detected multiple signals using time-resolve effect of optic switch.
- M-AOB had simplified structure and high sensitivity and light transmission effect.
- Two small molecules were simultaneously detected by M-AOB with high sensitivity.

GRAPHICAL ABSTRACT

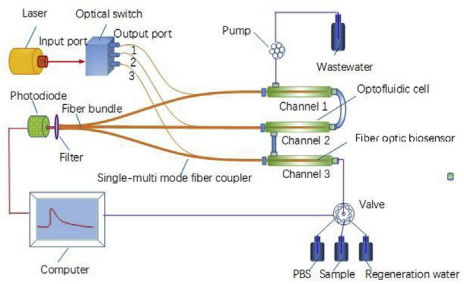

ARTICLE INFO

Article history:
Received 8 May 2018
Received in revised form
21 July 2018
Accepted 26 July 2018
Available online xxx

Keywords:
Evanescent wave biosensor
Small molecule
Optofluidic
Fiber optic coupler
Multitarget assay

ABSTRACT

An integrated multichannel all-fiber optofluidic biosensing platform (M-AOB) has been developed for a sensitive, rapid, and simultaneous detection of up to three trace analytes. The M-AOB platform employs a 1×3 fiber optical switch and three single-multimode fiber optic couplers for the transmission of excitation light and fluorescence and one photodiode detector for the simultaneous detection of fluorescence signals of multiple channels based on the time-resolve effect of the fiber optical switch. This design greatly simplified the entire system structure and improved light transmission efficiency. Through an indirect competitive immunoassay mechanism, we detected two highly regulated small molecules, namely, atrazine and 2,4-D, to demonstrate the value of M-AOB to the simultaneous measurement of trace analytes in water samples. The limits of detection of 0.03 μg/L and 0.04 μg/L were obtained for atrazine and 2,4-D, respectively, and were highly comparable with those of other analytical techniques. The high sensitivity of M-AOB benefited from the high light collective efficiency and low light loss of the excellent all-fiber optical structures and from the advantages of the evanescent wave technique. The regeneration of the biosensor surface, 200 assay cycles, were performed without any significant activity loss. Each assay cycle was less than 15 min. The immunoassay performance of the M-AOB, evaluated in several spiked water samples, showed good recovery, accuracy, and precision, indicating that the M-AOB was less susceptible to matrix effects of water samples. All these results illustrated that M-AOB can be readily extended toward the simultaneous and rapid detection of other trace small molecules using

* Corresponding author..
** Corresponding author. Research Institute of Chemical Defense, Academy of Military Sciences PLA China, Beijing, 102205, China..
E-mail addresses: longf04@ruc.edu.cn (F. Long), chuanna0306@163.com (A. Zhu).
[1] These authors contributed equally to this work.

https://doi.org/10.1016/j.aca.2018.07.067
0003-2670/

different biosensors modified by other analyte conjugates and their respective fluorescence-labeled antibodies.

1. Introduction

Microarray biosensors are powerful tools for high-throughput and rapid analysis of multiple analytes in low sample volumes [1–4]. Based on different signal transduction mechanisms, numerous optical, electrical, magnetic, thermal, and piezoelectric microarray biosensors have recently been designed for disease diagnosis, food surveillance, environmental monitoring, and drug development [2,3,5–7]. Optical microarrays, such as fiber optic array biosensors and biochips, have received considerable attention because of their unique characteristics, including high sensitivity, specificity, and excellent resistance to electromagnetic interference [6,8,9]. Despite the technological improvements made in the past decades, most of current microarray biosensor technologies lack portability and incapable of multiplexed, parallel, and automated analysis [2,3]. These limitations may be attributed to the following reasons: First, although the biorecognition elements of most biosensors are already miniaturized to microscale and even to nanoscale, their detection systems for these devices are macroscopic, expensive, and inflexible, and usually requires sophisticated and expensive optical design and coordination of light sources, detectors, and other subunits (e.g. off-axis parabolic reflector and biconvex silica lens) [3,10]. The use of high-technological equipment in these microarrays make them difficult to miniaturize and reduce operational costs, especially for multiplexed parallel measurements. Second, the entire system might be destroyed and difficult to reconvert when the directions of any optical elements become inaccurate. The reconfiguration of the optical detection systems is time-consuming, and very costly when the directions of any optical elements become inaccurate, and thus inconvenient for on-site detection. Third, a conventional microarray immobilizes captured antibodies/antigens as biorecognition elements onto a heterogeneous biochip (e.g., glass slide) by microprinting or microstructuring processes. These fabrications require expensive equipment and multiple steps, which are labor intensive and prone to variability owing to immobilization chemistry, spotting buffer, and environmental conditions [11,12]. Therefore, the challenges still remain to develop novel microarray biosensors that are portable, capable of multiplexed and automated analysis, high sensitive, and easy to operate and exhibit good regenerable performance without using expensive equipment and complex operation conditions. It is highly desirable to develop integrated, simple yet efficient optical detection system in optofluidic biosensing platform to overcome the existing challenges.

Evanescent wave fiber-optical microarray biosensors have received considerable attention because of their small size, good flexibility, low propagation loss, and high sensitivity and specificity [13]. Since the first use of evanescent wave excitation for fluorescence immunoassay by Kronick and Little [14], several evanescent wave-based fiber optic biosensors have been proposed and applied for the determination of trace targets on the basis of total internal reflect fluorescence [3,15,16]. For instance, RAPTOR and Analyte 2000, both fiber-optical microarray biosensors, had successfully been applied for the detection of multiple bacteria and organic pollutants [17–19]. However, these microarray biosensors had complex optical systems with rigorous optical alignment. Moreover, the biosensor was consisted of plastic fiber optic with special structure, and the antibody were immobilized onto the biosensor surface as biorecognition element, resulting in a poor regeneration performance. Our group previously developed an evanescent wave all-fiber biosensor by using a single-multimode fiber optic structure to achieve the transmission of the excitation light and fluorescence [16]. The entire system was simple, portable, and highly sensitive. This biosensor had been applied for the detection of environmental pollutants and biological samples [16,20]. Furthermore, optofluidic platforms, integrated with photonics and microfluidics, are rapidly becoming useful in biosensor instruments because of their unique capabilities, which include simplification of the microsystem designs, enhancement of sensing performances, and reduction of sample volumes [21,22]. Evanescent wave-based technologies have become one of the most successful optofluidic platforms because of the limited penetration depths of evanescent waves [23]. The evanescent wave generated at the optical waveguide surface, decaying exponentially with distance, penetrates essentially into the surrounding cladding of lower refractive index and has a typical penetration depth of 100–200 nm. This penetration depth enables optical interactions between the optical waveguide and biomolecules bound to the waveguide surface. Thus, investigating biomolecular interactions on optofluidic-based biosensing surfaces becomes effortless [24].

To address these questions and integrate the advantages of optofluidic and all-fiber optical structure, an integrated multichannel all-fiber optofluidic biosensing platform (M-AOB) was fabricated with a 1×3 fiber optical switch and three single-multimode fiber optic couplers for the transmission of excitation light and collection and transmission of fluorescence. In this platform, one photodiode detector was used for the simultaneous detection of fluorescence signals of multiple channels based on the time-resolved effect of the fiber optical switch. The all-fiber structure of the M-AOB not only reduced the required optical components and rigorous optical alignment but also improved the light transmission, fluorescence collection efficiency, and signal-to-noise ratio. Through the control of a ten-way valve and pump, the samples could be automatically introduced into the optofluidic cells and rapidly be detected through a programmed procedure. Moreover, the use of three split optofluidic cells enabled the detection of a single target or the simultaneous detection of multiple targets. These designs rendered the entire system simple, compact, flexible, automatic, and miniaturized. Based on the principle of total internal reflection fluorescence and indirect competitive immunoassay, we detected two highly regulated small molecules, namely, atrazine and 2,4-D, by using the M-AOB. The sensitivity, specificity, reusability, and accuracy of this platform were also evaluated.

2. Technical design of M-AOB

The novel integrated multichannel all-fiber optofluidic biosensing platform was developed through a modular approach. The final device comprised four technical parts, namely, the optical system, optofluidic cell, fluidics, and mini-computer, which controlled the device and processes the results, as shown in Fig. 1.

To simplify the structure of our platform, we used a 1×3 microelectron mechanical-based fiber optical switch (Thorlabs, USA) and three single-multimode fiber optic couplers, which were

Please cite this article in press as: W. Li, et al., Integrated multichannel all-fiber optofluidic biosensing platform for sensitive and simultaneous detection of trace analytes, Analytica Chimica Acta (2018), https://doi.org/10.1016/j.aca.2018.07.067

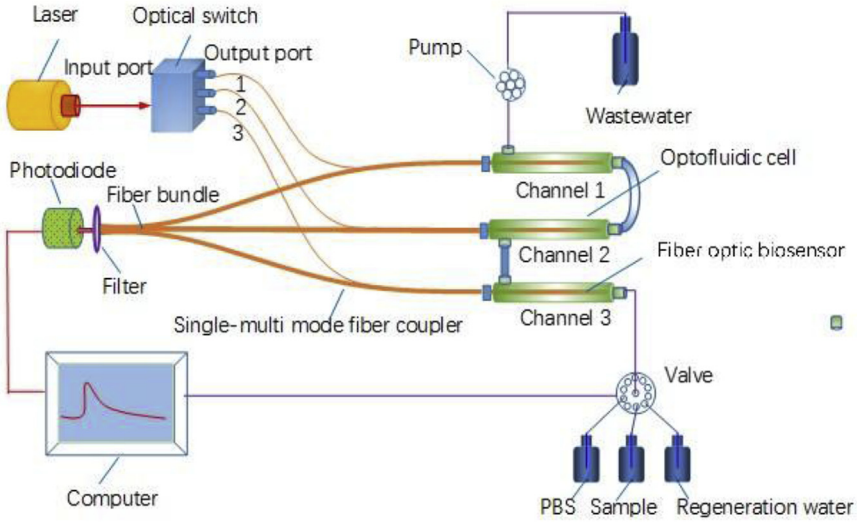

Fig. 1. Scheme of the M-AOB system: the optical system (laser, fiber optical switch, single-multimode fiber optic coupler, filter, and photodiode detector), the optofluidic system (optofluidic cells and biosensors), the fluidics (pump and valve), and a mini-computer.

key elements of the optical system in the M-AOB, to transfer excitation light and collect fluorescence signals (Fig. 1). The fiber optical switch exhibited low crosstalk, long lifetime, low insertion loss, fast switching time (typ 0.5 m s), and excellent repeatability and had one input port and three output ports. A single-mode optical fiber jumper was used for linking the input port of the switch with a 635 nm laser diode (adjustable power as required), which was selected as an excitation light source. Software was used for the control of the excitation light output from any of the three output ports of the fiber optical switch. Furthermore, the switching interval from one output port to another output port may be set from 0.1 s to 10 s. In our system, the switching interval was set as 1 s, and a sequential switching method (1-2-3-1-2-3-1 … …) was applied. However, each output port of the fiber optical switch was linked with a single-mode fiber of the single-multimode fiber coupler. In the M-AOB system, three single-multimode fiber couplers were used to transfer excitation light and collect fluorescence signals (Fig. 1). One end of the multimode fiber, with a 600 μm diameter (NA = 0.22) coupler, was linked with a fiber optic biosensor. However, the other end of three multimode fibers of the coupler that shared a photodiode detector was combined into a fiber bundle. In our M-AOB, other separated optical elements, such as lens and dichroic mirror, are unnecessary, and thus the requirement of rigorous optical alignment was reduced, and the efficiency of light transmission and signal-to-noise ratio were improved.

The excitation light from an output port of the fiber optical switch entered into one biosensor through the multimode fiber of one single-multimode fiber coupler and was transmitted in the biosensor in the form of total internal reflection. The evanescent wave, generated on the biosensor surface, excited fluorescence dye primarily from the fluorescence-labeled antibodies bound to the biosensor surface through affinity recognition interactions. Parts of fluorescence coupled back into the biosensor and were transmitted into the multimode fiber through the fiber connector. The collected fluorescence, which was filtered with a bandpass filter (FF01-692/40, Semrock, USA) to reject any lost and scattered laser light, was detected by the photodiode detector. When the laser light outputted in turn from three ports of the fiber optical switch, the fluorescence bound onto each biosensor surface in each channel was sequentially excited and collected by its corresponding multimode fiber and was successively detected by the same photodiode detector. Given the time-resolved effect of the fiber optical switch, the fluorescence from three separated biosensors could be detected real-time by one photodiode detector, whereas three fluorescence signal traces were simultaneously demonstrated on the user interface. As we known, the fluorescence lifetime of Cy5.5 is typically nanoseconds. Therefore, our detector coould easily discriminate the fluorescence signal from each channel using time-resolved effect of fiber optical switch.

The combined tapered fiber optic biosensor, produced by our previous developed method,[16] was embedded in each optofluidic cell. The fluids (e.g. samples, buffer) in the M-AOB system was introduced into the optofluidic cells by a six-roller peristaltic pump, which smoothly moved the liquid in a flow rate of 5–1000 μL/min. The type of input fluid medium was selected by a multiposition solenoid valve (VICI Valco, Interchim) with ten inlet ports and one outlet port. These two elements were controlled via an RS232 port on a computer interface through a programmed procedure. The measurement cycles, including baseline detection, sample detection, and regeneration process, could be programmed via a user interface. The detection software system, developed with visual C^{++} 6.0, was capable of displaying real-time data graphics and saving and opening measured data. Experimental parameters, such as switching interval time, analysis and regeneration sequences, flow rate, and number of detection channels could be configured through the user interface.

3. Experimental sections

3.1. Reagents and chemicals

Atrazine, 2,4-D, Glutaraldehyde (GA), (3-Aminopropyl)-trimethoxysilane (APTES), and bovine serum albumin (BSA) were purchased from Sigma-Aldrich. H_2SO_4, H_2O_2, and all other reagents, unless specified, were supplied by Beijing Chemical Agents. All reagents were used as received. Distilled deionized water was used throughout the investigation. 0.01 M phosphate buffer solution (PBS, pH = 7.4) was used. 0.5% sodium dodecyl sulfate (SDS, pH = 1.9) was applied to regenerate the biosensor.

Monoclonal anti-Atrazine and anti-2,4-D antibody, atrazine-OVA, and 2,4-D-OVA were produced by our research group, and two antibodies (anti-mouse IgG) were labeled by Cy5.5.100 μg/mL atrazine stock solutions and 100 μg/mL 2,4-D stock solutions were prepared in methanol and stored at 4 °C, respectively. The atrazine

Please cite this article in press as: W. Li, et al., Integrated multichannel all-fiber optofluidic biosensing platform for sensitive and simultaneous detection of trace analytes, Analytica Chimica Acta (2018), https://doi.org/10.1016/j.aca.2018.07.067

and 2,4-D standard solutions were prepared from the stock solution by serial dilutions in PBS.

3.2. Biosensor functionalization

The biosensor was functionalized to detect small molecules (e.g., 2,4-D and atrazine) according to the previously described method [25,26]. The hapten-carrier protein conjugates (atrazine-OVA or 2,4-D-OVA), served as bio-recognition molecules, were immobilized onto the silanized optical fiber biosensor surface using the heterobifunctional crosslinker coupling strategy. Details were shown in supporting information (Fig. S1).

3.3. Data analysis

Dose-response curves were measured for immunoassay of small molecules. All values obtained in the following plots represent the mean values of three measurements and their standard deviation. Curves were fitted with a four-parameter logistic model as following.

$$y = \frac{A_1 - A_2}{1 + ([Ag]/[Ag_0])^P} + A_2 \quad (1)$$

Where (Ag) is the small molecule concentration; A_1 and A_2 are the upper and lower asymptote (background signal) to the dose-response curve; (Ag_0) is the small molecule concentration at inflection; and p is the slope at the inflection point.

4. Results and discussions

4.1. Characteristic of M-AOB platform

We investigated the response signals on the three sensors at the same concentration of 2 μg/mL Cy5.5-labeled anti-2,4-D antibody solution. The biosensor in Channel 1 was modified by 2,4-D-OVA, whereas the other two sensors in Channels 2–3 were unmodified fiber optic probe. The results were shown in Fig. 2. When Cy5.5-labeled anti-2,4-D antibody solution was introduced into the optofluidic cells, the fluorescence signal rapidly increased in Channel 1, which contributed to fluorescence-labeled antibody, specifically bound to the hapten conjugates that were immobilized onto the sensor surface. However, only a little fluorescence signal in the other two channels was detected, indicating that few non-specific adsorption of free Cy5.5 occurred on the sensor surface, and the free dye molecules in the bulk solution was less excited by the evanescent wave. These results contributed to the decay length of the evanescent field on the sensor surface in the nanometer scale. The abrupt signal enhancement of the signal trace in channel 1 and 2 should contribute to the existence of air bubbles when the sample or regeneration solution was introduced into the sample cell. The uniformity of three channels was also investigated. The relative standard deviation of baseline signals without fluorescence dye for different sensors was 5.3% (Fig. 2-I). After the regeneration of biosensor in Channel 1, the signal value returned to the baseline, and the relative standard deviation of baseline signals from Channels 1–3 was 6.4% (Fig. 2-II). Moreover, when three biosensors modified by 2,4-D-OVA were respectively placed in Channels 1–3, the fluorescence signals in three channels were similar after the fluorescence labeled anti-2,4-D antibody was introduced (Fig. S2), and the standard deviation of peak values was 5.9%. This slight non-uniformity of M-AOB signal in various channels was acceptable and did not affect the immunoassay since all measurements were normalized, with respect to the blank signal at their respective channels (See Section 4.2). All results indicated that the M-AOB platform was suitable to be used for the surface-based immunoassay of multitargets.

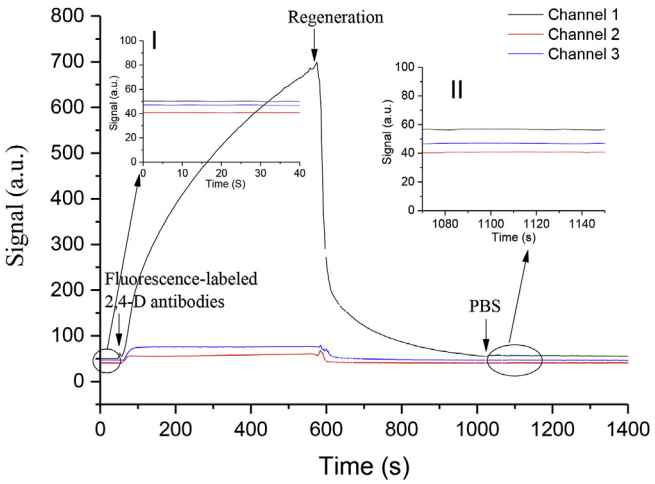

Fig. 2. The response trace signal of Cy5.5-labeled anti-2,4-D antibody (2.0 μg/mL) in three channels (Channel 1: 2,4-D-OVA-modified biosensor and Channel 2–3: unmodified fiber optic sensors). Inset I: Baselines of three channels before sampling. Inset II: Baselines of three channels after regeneration.

Furthermore, a good regeneration performance of the biosensor surface, immobilized by bio-recognition moles, is a desired feature for biosensors in practical application. For this, a large number of immunoassays (taking 2,4-D for example) were performed to evaluate the stability and activity of the immobilized immunosurface (Fig. S3). The biorecognition elements could retain at least 200 successive assays without loss of activity, and the decrease in the average maximum signal response of small molecule specific antibodies with the absence of analyte was less than 8.2%. After each determination cycle, the non-covalently bound antibodies was completely removed, and the active sensor surface was completely regenerated. Good regeneration performance, excellent binding properties, and robustness of the biosensor surface in the proposed biosensing platform ensured the cost-effective, sensitive, and accurate measurement of small analytes.

4.2. Biosensing mechanism for the simultaneous detection of small molecules

Taking two channels for example, we demonstrated the simultaneous immunoassay mechanisms of two small molecules, atrazine and 2,4-D as the model analytes, using the proposed optofluidic biosensing platform (Fig. 3A). 2,4-D and Atrazine, two of the most heavily used herbicides worldwide, pose a potential health risk to humans and to wildlife even at very low levels and may lead to the occurrence of cancer and endocrine-disrupting activities [27,28]. These analytes are high concerns and have been routinely detected in surface and drinking water because of its moderate solubility and relative persistence.

To simultaneously detect atrazine and 2,4-D, we embedded the biosensors immobilized by atrazine-OVA and 2,4-D-OVA in Channels 1 and 2, respectively. Indirect competitive immunoassay mechanism was applied to detect two small molecules. Fig. 3B illustrate the exemplary real-time fluorescence signal trace of two small analytes using M-AOB platform. One analysis cycle includes three steps. First, 0.3 mL of samples containing various concentrations of small molecules were mixed and pre-reacted with 0.3 mL of fluorescence-labeled antibodies at a fixed concentration for a certain time (also called pre-incubation). During this time, the

Please cite this article in press as: W. Li, et al., Integrated multichannel all-fiber optofluidic biosensing platform for sensitive and simultaneous detection of trace analytes, Analytica Chimica Acta (2018), https://doi.org/10.1016/j.aca.2018.07.067

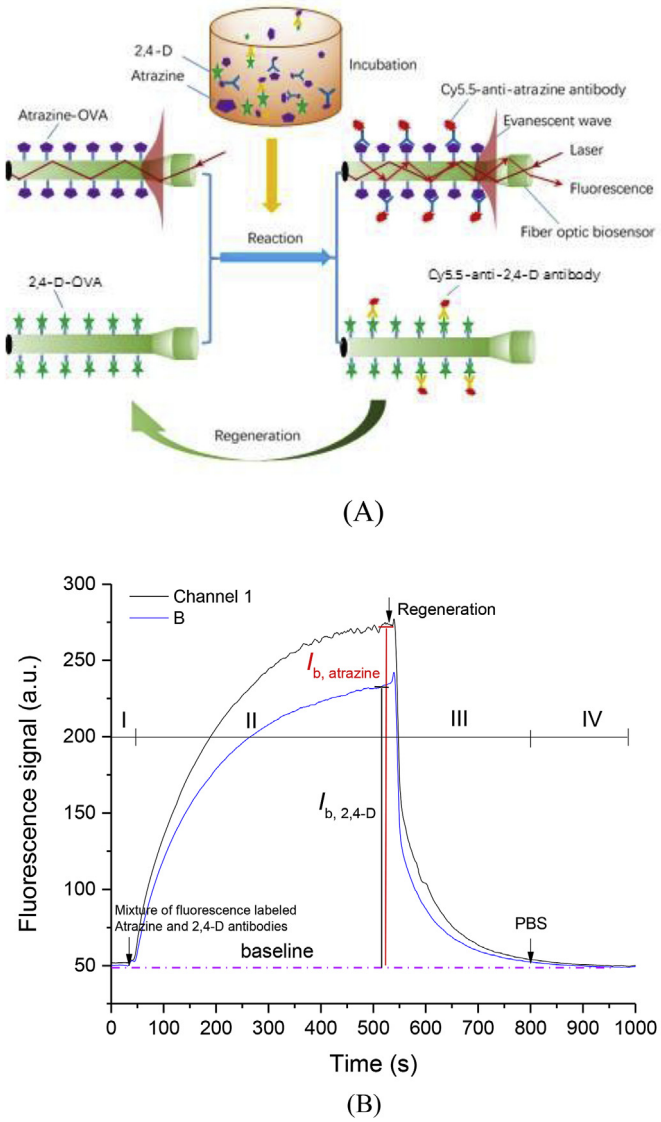

Fig. 3. (A) Schematic of biosensing mechanism for the simultaneous detection of small molecules (atrazine and 2,4-D). (B) Representative signal profile for simultaneous detection of atrazine and 2,4-D using the M-AOB. The mixture of 1.0 μg/mL fluorescence-labeled anti-atrazine and anti-2,4-D antibodies was introduced into the optofluidic cells. The biosensors immobilized by atrazine-OVA and 2,4-D-OVA were placed in channel 1 and 2, respectively.

portion of anti-small molecule antibodies specifically bound to small molecules and the occupied antibody binding sites were proportional to the concentration of small molecules in the samples. Then, the mixture was delivered to the optofluidic cell. The fluorescence-labeled antibodies with remaining binding sites were able to bind to the coating-antigen conjugates immobilized onto the fiber optic biosensor surface (Phase II in Fig. 3B). The surface-bound Cy5.5-labeled antibodies were excited in the evanescent field, and the fluorescence signal was real-time recorded, which was also undertaken as binding occurred between antibodies, with free binding sites and immobilized hapten of the biosensors (Phase II in Fig. 3B). Finally, the biosensing surface was regenerated with 0.5% SDS solution (pH 1.9) to break the antibody-antigen association (Phase III in Fig. 3B). The sample was then washed with PBS solution (Phase IV in Fig. 3B). The regenerated biosensors were ready for the next test. To reduce the test time, the fluorescence signal value of 6 min, which was about 80% of a maximum, was regarded as the effective result.

For each assay, the net fluorescence intensity *(I)* for the subsequent determination of dose-response relationships were calculated by subtracting the baseline signal value according to Eq. (2):

$$I = \text{Signal value after the 6 min reaction} - \text{Signal value at the baseline} \quad (2)$$

The normalized response was calculated according to Eq. (3):

$$I_n = \Delta I / I_b = (I_b - I_s)/ I_b \text{ (a.u. fluorescence intensity)} \quad (3)$$

Where, I_b is the net fluorescent intensity of the blank in the absence of small molecules, and I_s the net fluorescent intensity of the samples in the presence of small molecules.

4.3. Cross-reactivity of multichannel detection

Cross-reactivity is an important analytical parameter regarding specificity and reliability of immunoassays, especially for simultaneous detection of several targets. Several control experiments were conducted to evaluate the cross-reactivity of the simultaneous detection of atrazine and 2,4-D. First, 1.0 μg/mL of fluorescence-labeled anti-atrazine antibody was introduced into the optofluidic cells (Fig. 4A). After 500 s, a strong fluorescent signal was detected in Channel 1, which indicates binding of the anti-atrazine antibody to the biosensor surface. However, a little fluorescent signal was observed in Channel 2, indicating no obvious non-specific adsorption of anti-atrazine antibody onto the

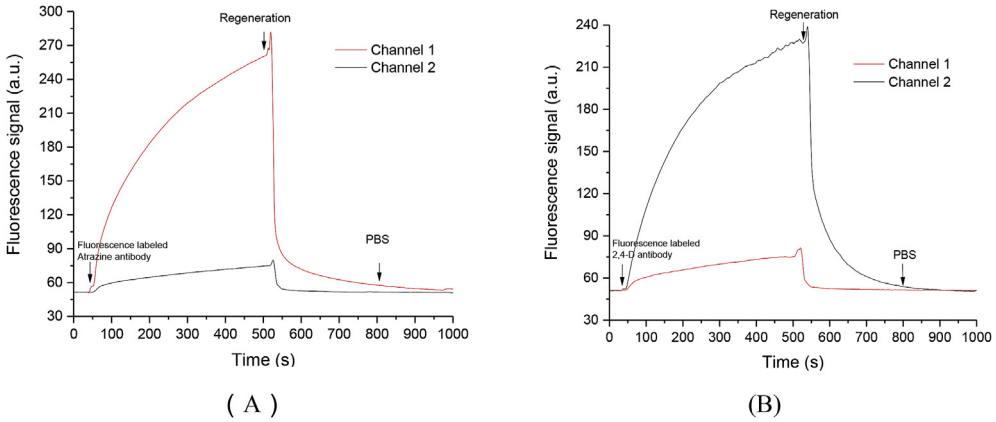

Fig. 4. Assessment of the specific binding between fluorescence-labeled specific antibodies and their antigens. (A) Experiment with 1.0 μg/mL of fluorescence-labeled anti-atrazine antibodies introduced into Channels 1 and 2; (B) Experiment with 1.0 μg/mL of fluorescence-labeled anti-2,4-D antibodies introduced into Channels 1 and 2.

Please cite this article in press as: W. Li, et al., Integrated multichannel all-fiber optofluidic biosensing platform for sensitive and simultaneous detection of trace analytes, Analytica Chimica Acta (2018), https://doi.org/10.1016/j.aca.2018.07.067

biosensor surface modified by 2,4-D-OVA. Second, 1.0 μg/mL of fluorescence-labeled anti-2,4-D antibody was delivered into the optofluidic cells (Fig. 4B). After 500 s, a strong fluorescent signal was detected in Channel 2, indicating binding of the anti-2,4-D antibody to the biosensor surface. Likewise, a little fluorescent signal was observed in Channel 1, indicating no obvious non-specific adsorption of anti-2,4-D antibody onto the biosensor surface modified by atrazine-OVA. Third, the mixture of 1.0 μg/mL fluorescence-labeled anti-2,4-D and atrazine antibody were simultaneously introduced to both of biosensor surface (Fig. 3B); the strong fluorescence signals were observed in Channels 1 and 2. These results confirmed that the observed fluorescence signal originated from the special binding between atrazine-OVA or 2,4-D-OVA immobilized onto the biosensor surface and the fluorescence-labeled anti-atrzine and anti-2,4-D antibodies, respectively. The results demonstrated that anti-atrazine and anti-2,4-D antibody exhibited high specificity for atrazine and 2,4-D, respectively. These results demonstrated a high ability of the biosensor in detecting the binding between specific antibody and its antigen, and also proved that the non-specific adsorption of antibody onto the biosensor surface was negligible.

4.4. Dose-response curves of atrazine and 2,4-D immunoassay

To perform indirect competitive immunoassay, the atrazine and 2,4-D solutions of various concentrations, ranging from 0 μg/L to 1000 μg/L, were mixed with 2.0 μg/mL of anti-2,4-D antibody and 2.0 μg/mL of anti-atrazine antibody (v/v, 1:1). The mixture was incubated for 5 min. During this process, the binding sites of the anti-atrazine antibody or anti-2,4-D antibody were occupied according to the concentration of atrazine or 2,4-D, respectively. Then, the mixture was sequentially introduced over Channel 1 (biosensor immobilized by atrazine-OVA), Channel 2 (biosensor immobilized by 2,4-D-OVA), and Channel 3 (unmodified sensor) at a flow-rate of 200 μL/min. The reaction time was 5 min, and the fluorescence signals of three channels were simultaneously recorded. The typical fluorescence signal values were shown in Fig. 5A, and the fluorescence traces of Channel 1 and Channel 2 were shown in Fig. S4. With the increase of the concentration of analytes in the sample, less fluorescence-labeled antibodies were bound to modified hapten onto the biosensor surface, resulting in a lower fluorescent signal detected by biosensing platform. In the control channel, few fluorescence signals were detected no matter how much the concentration of two pesticides was added. Afterwards, regeneration of the biosensor surface was carried out by using 0.5% SDS (pH 1.9) and then rinsing with PBS. A complete test-cycle took about 15 min for completion (Fig. S4).

The dose-response curves of atrazine and 2,4-D, normalized by expressing the signal of each standard point as the ratio of the maximum response according to Eq. (3), were shown in Fig. 5. The logistic dose-response curves were used to fit the parallel titration of atrazine and 2,4-D, respectively. The linear responses in the range of 0.15 μg/L to 108.50 μg/L and 0.10 μg/L to 102.50 μg/L were for atrazine and 2,4-D, respectively. The limits of detection (LOD), using three standard deviation of the mean blank values, were 0.03 μg/L and 0.04 μg/L for atrazine and 2,4-D, respectively. The LOD met the requirements for the determination of pesticides in drinking water demanded by the European Union. In Europe legislation, the limits of pesticide concentration in drinking water are 0.1 μg/L for a single substance and 0.5 μg/L for the sum of all pesticides [29]. Although a number of biosensors have been reported for the detection of atrazine and 2,4-D, most of them only detected one pesticide in one cycle and involved laborious time-consuming procedures, trained personnel, or laboratory-based expensive instrumentations [27,30,31]. Furthermore, the performance of the established optofluidic biosensing platform was highly comparable with those obtained through other analytical techniques [27,28,30–33]. The results confirmed the application prospects of the proposed M-AOB for achieving the simultaneous detection of several contaminants in one sample.

4.5. Spiked water analysis

The evaluation of matrix effects is essential in assessing newly developed immunoassay methods because the binding of antibody

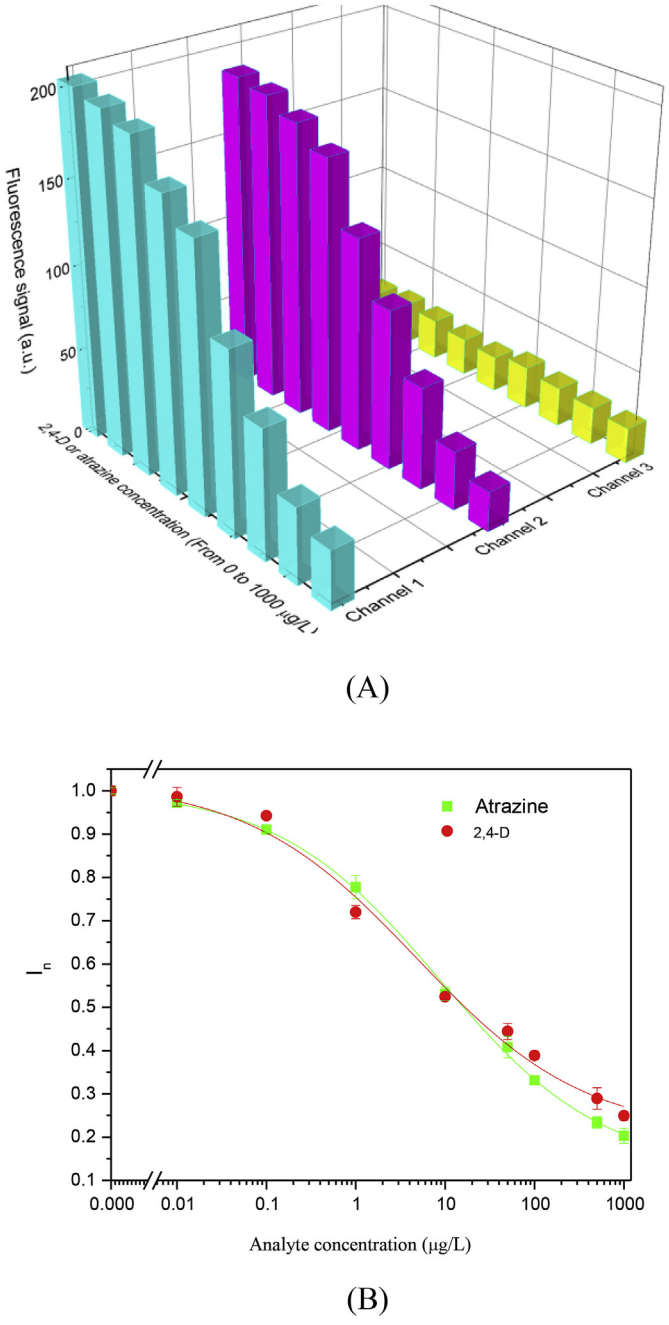

Fig. 5. (A) The typical fluorescence signal values in three channels. The biosensors immobilized by atrazine-OVA and 2,4-D-OVA were placed in Channel 1 and Channel 2, respectively, and the unmodified sensor was placed in Channel 3. (B) Logistic-fitted calibration curves for atrazine and 2,4-D determination using the M-AOB, and the error bars corresponded to the standard deviation of the data points in three repeated experiments (n = 3).

Please cite this article in press as: W. Li, et al., Integrated multichannel all-fiber optofluidic biosensing platform for sensitive and simultaneous detection of trace analytes, Analytica Chimica Acta (2018), https://doi.org/10.1016/j.aca.2018.07.067

Table 1
Recovery of M-AOB towards atrazine and 2, 4-D in water samples (n = 3).

Samples	Targets	Spiked (μg/L)	Measured (μg/L)	Recovery (%)	CV (%)
Tap water	2,4-D	0.1	0.09	90	3.42
		1.0	1.12	112	4.81
		10.0	10.95	110	3.11
	Atrazine	2.0	1.96	98	2.43
		5.0	5.5	110	3.24
		10.0	10.47	105	4.95
The Old Summer Palace	2,4-D	0.1	0.11	110	5.62
		1.0	1.12	112	4.35
		10.0	10.76	108	5.24
	Atrazine	2.0	1.78	89	2.94
		5.0	5.8	116	2.98
		10.0	10.56	106	6.65
Beihai Lake	2,4-D	0.1	0.1	100	3.49
		1.0	1.07	107	2.12
		10.0	9.33	93	6.01
	Atrazine	2.0	2.26	113	1.69
		5.0	5.34	107	5.34
		10.0	9.68	97	9.68

*Atrazine and 2,4-D were not detected from all original water samples.

and antigen is affected by matrix effects (e.g. pH, ionic strength, etc.) in real samples [34,35]. Herein, a recovery study was performed using several real water samples, including lab tap water and water samples from the Old Summer Palace and Beihai Lake. These environmental samples were spiked with atrazine or 2,4-D from their stock solution at various concentrations. Then, the atrazine or 2,4-D content were measured according to the procedure described (in triplicates), and the results were summarized in Table 1. Satisfactory recoveries were obtained within the linear concentration range. The average recoveries of the spiked samples varied from 80% to 120%. Parallel test results showed that the coefficient of variation (CV) was not more than 10%. These results definitely demonstrated that any possible interference from the different background compositions of real water samples on the optofluidic biosensing analysis was negligible. The accuracy and reliability of the present method confirmed the application potential of the M-AOB to simultaneously measure several trace analytes in real water samples.

5. Conclusions and outlooks

An integrated multichannel all-fiber optofluidic biosensing platform was developed for a sensitive, cost-effective, rapid, and simultaneous detection of trace analytes. The constructed prototype set-up comprised four technical parts, namely, the optical system, optofluidic cell, fluidics, and computer interface. The key parts of the M-AOB platform were the 1×3 optical switch and three single-multimode fiber optic couplers for excitation light and fluorescence transmission, and one photodiode detector for the simultaneously detection of fluorescence signals of multiple channels through the time-resolve effect of the fiber optical switch. These structures allowed the M-AOB to have a simple optical alignment, and thus be simple, compact, flexible, and miniaturized.

Another important aim of this study was to demonstrate the value of M-AOB in the simultaneous measurement of trace analytes in water samples. In the proof-of-concept experiment, two highly regulated small pollutants (atrazine and 2,4-D) were simultaneously detected through an indirect competitive immunoassay mechanism with high sensitivity and specificity. More than 200 assay cycles were performed without significant activity loss owing to the regeneration of the biosensor surface. The immunoassay performance of the M-AOB evaluated in several spiked water samples showed good recovery, accuracy, and precision, indicating less susceptibility of M-AOB to the matrix effects of water samples. We will simultaneously detect more targets using this platform in the next experiments.

Compared with other optic fiber-based array biosensors [15,23], the developed M-AOB was obviously more advantageous because its structure was simple, compact, inexpensive to produce, and easy-to-operate, and it had good regeneration and miniaturization features. Our current biosensing platform could simultaneously detect up to three different targets through the addition of biosensors modified by various hapten-conjugates and respective fluorescence-labeled antibodies. Moreover, selecting channel numbers to meet the detection requirement of different numbers of targets could be flexible. In the future, if more output port-based fiber optical switch and more single-multi mode fiber couplers were used, more detection channels could be obtained, resulting in that more targets could simultaneously be detected in one-assay cycle. Owing to its capability to rapidly and simultaneously detect small analytes, M-AOB has great potential application in disease diagnosis, drug discovery, food safety, and environmental monitoring, especially in individual laboratories and clinics in developing countries.

Notes

The authors declare no conflicts of interest.

Acknowledgment

This research was financially supported by the National Natural Science Foundation of China (21675171, 21277173), the National Instrument Major Project of China (2012YQ3011105), the Fundamental Research Funds for the Central Universities, and the Research Funds of Renmin University of China (15XNLD04), and the Special Fund of State Key Joint Laboratory of Environment Simulation and Pollution Control (17K06ESPCT).

Appendix A. Supplementary data

Supplementary data related to this article can be found at https://doi.org/10.1016/j.aca.2018.07.067.

References

[1] R. Niessner, M. Seidel, Automated analytical microarrays: a critical review,

Anal. Bioanal. Chem. 391 (2008) 1521–1544.
[2] A.P.F. Turner, Biosensors: sense and sensibility, Chem. Soc. Rev. 42 (2013) 3184–3196.
[3] X.D. Wang, O.S. Wolfbeis, Fiber-optic chemical sensors and biosensors (2013–2015), Anal. Chem. 85 (2016) 203–227.
[4] S. Herranz, M. Marciello, P.M. Marco, L.J. Garcia-Fierro, M.J. Guisan, C.M. Moreno-Bondi, Multiplex environmental pollutant analysis using an array biosensor coated with chimeric hapten-dextran-lipase constructs, Sens. Actuators, B 257 (2018) 256–262.
[5] U. Rant, K. Arinaga, S. Scherer, E. Pringsheim, S. Fujita, N. Yokoyama, et al., Switchable DNA interfaces for the highly sensitive detection of label-free DNA targets, Proc. Natl. Acad. Sci. Unit. States Am. 104 (2007) 17364–17369.
[6] L. Liu, X. Zhou, M. Lu, M. Zhang, C. Yang, R. Ma, et al., An array fluorescent biosensor based on planar waveguide formulti-analyte determination in water samples, Sensor. Actuator. B Chem. 240 (2017) 107–113.
[7] T. Chen, G. Cheng, S. Ahmed, Y. Wang, X. Wang, H. Hao, et al., New methodologies in screening of antibiotic residues in animal-derived foods: Biosensors, Talanta 175 (2017) 435–442.
[8] A. Leung, P.M. Shankar, R. Mutharasan, A review of fiber-optic biosensors, Sensor. Actuator. B Chem. 125 (2007) 688–703.
[9] L. Liu, X. Zhou, J.S. Wilkinson, P. Hua, B. Song, H. Shi, Integrated optical waveguide-based fluorescent immunosensor for fast and sensitive detection of microcystin-LR in lakes: optimization and analysis, Sci. Rep. 7 (2017) 3655.
[10] P. Teerapanich, M. Pugnière, C. Henriquet, Y.L. Lin, C.F. Chou, T. Leïchlé, Nanofluidic Fluorescence Microscopy (NFM) for real-time monitoring of protein binding kinetics and affinity studies, Biosens. Bioelectron. 88 (2016) 25–33.
[11] N. Ramachandran, E. Hainsworth, B. Bhullar, S. Eisenstein, B. Rosen, A.Y. Lau, et al., Self-assembling protein microarrays, Science 305 (2004) 86–90.
[12] C. Wingren, C.A.K. Borrebaeck, Antibody microarrays: current status and key technological advances, J. Integr. Biol. 10 (2006) 411–427.
[13] C.R. Taitt, G.P. Anderson, F.S. Ligler, Evanescent wave fluorescence biosensors, Biosens. Bioelectron. 20 (2005) 2470–2487.
[14] M.N. Kronick, W.A. Little, A new immunoassay based on fluorescenceexcitation by internal reflection spectroscopy, J. Immunol. Meth. 8 (1975) 235–240.
[15] F.S. Ligler, C.R. Taitt, L.C. Shriver-Lake, E.K. Sapsford, Y. Shubin, P.J. Golden, Array biosensor for detection of toxins, Anal. Bioanal. Chem. 377 (2003) 469–477.
[16] F. Long, M. He, H.C. Shi, A.N. Zhu, Development of evanescent wave all-fiber immunosensor for environmental water analysis, Biosens. Bioelectron. 23 (2008) 952–958.
[17] C.C. Jung, E.W. Saaski, D.A. McCrae, B.M. Lingerfelt, G.P. Anderson, RAPTOR: a fluoroimmunoassay-based fiber optic sensor for detection of biological threats, IEEE Sensor. J. 3 (2003) 352–360.
[18] G.P. Anderson, B.M. Lingerfelt, C.R. Taitt, Evaluation of optical detection platforms for multiplexed detection of proteins and the need for point-of-care biosensors for clinical use, Sens. Lett. 2 (2004) 1–7.
[19] S.D. Leskinen, D.V. Lim, Rapid ultrafiltration concentration and biosensor detection of enterococci from large volumes of Florida recreational water, Appl. Environ. Microbiol. 74 (2008) 4792–4798.
[20] Y. Tang, F. Long, C. Gu, C. Wang, S. Han, M. He, Reusable split-aptamer-based biosensor for rapid detection of cocaine in serum by using an all-fiber evanescent wave optical biosensing platform, Anal. Chim. Acta 933 (2016) 182–188.
[21] X. Fan, M.I. White, Optofluidic microsystems for chemical and biological analysis, Nat. Photon. 5 (2011) 591–597.
[22] K.E. Sackmann, L.A. Fulton, J.D. Beebe, The present and future role of microfluidics in biomedical research, Nature 507 (2014) 181–189.
[23] R.C. Taitt, P.G. Anderson, S.F. Ligler, Evanescent wave fluorescence biosensors: advances of the last decade, Biosens. Bioelectron. 76 (2016) 103–112.
[24] S.M. Harazim, V.A. Bolanös, S. Kiravittaya, S. Sanchez, O.G. Schmidta, Lab-in-a-tube: on-chip integration of glass optofluidic ring resonators for label-free sensing applications, Lab a Chip 12 (2012) 2649–2655.
[25] F. Long, M. He, A.N. Zhu, H.C. Shi, Portable optical immunosensor for highly sensitive detection of microcystin-LR in water samples, Biosens. Bioelectron. 24 (2009) 2346–2351.
[26] S.K. Bhatia, L.C. Shriver-Lake, K.J. Prior, J.H. Georger, J.M. Calvert, R. Bredehorst, et al., Use of thiol-terminal silanes and heterobifunctional crosslinkers for immobilization of antibodies on silica surfaces, Anal. Biochem. 178 (1989) 408–413.
[27] X. Wang, J. Yu, X. Wu, J. Fu, Q. Kang, D. Shen, et al., A molecular imprinting-based turn-on Ratiometric fluorescence sensor for highly selective and sensitive detection of 2,4-dichlorophenoxyacetic acid (2,4-D). Biosens, Bioelectron 81 (2016) 438–444.
[28] N. Belkhamssa, I.L.C. Justino, S.M.P. Santos, S. Cardoso, I. Lopes, C.A. Duarte, et al., Label-free disposable immunosensor for detection of atrazine, Talanta 146 (2016) 430–434.
[29] F. Matsumura, International Encyclopedia of Pharmacology and Therapeutics, Pergamon Press, New York, 1994, p. 453 (Section 113).
[30] B. Danielsson, I. Surugiu, A. Dzgoev, M. Mecklenburg, K. Ramanathan, Optical detection of pesticides and drugs based on chemiluminescence–fluorescence assays, Anal. Chim. Acta 426 (2001) 227–234.
[31] K.V. Gupta, L.M. Yola, T. Eren, N. Atar, Selective QCM sensor based on atrazine imprinted polymer: its application to wastewater sample, Sens. Actuators, B 218 (2015) 215–221.
[32] J. Kaur, K.V. Singh, A.H. Schmid, G.C. Varshney, C.R. Suri, M. Raje, Atomic force spectroscopy-based study of antibody pesticide interactions for characterization of immunosensor surface, Biosens. Bioelectron. 20 (2004) 284–293.
[33] L. Liu, D. Shan, X. Zhou, H. Shi, B. Song, F. Falke, A. Leinse, R. Heideman, TriPleX™ waveguide-based fluorescence biosensor for multichannel environmental contaminants detection, Biosens. Bioelectron. 106 (2018) 117–121.
[34] L. Liu, X. Zhou, R. Ma, M. He, H. Shi, Y. Qian, High-throughput biomolecular interaction analysis probing by an array fluorescent biosensor platform, Sensor. Actuator. B Chem. 259 (2018) 888–893.
[35] E. Yılmaz, E. Özgür, N. Bereli, D. Türkmen, A. Denizli, Plastic antibody based surface plasmon resonance nanosensors for selective atrazine detection, Mater. Sci. Eng. C 73 (2017) 603–610.

Please cite this article in press as: W. Li, et al., Integrated multichannel all-fiber optofluidic biosensing platform for sensitive and simultaneous detection of trace analytes, Analytica Chimica Acta (2018), https://doi.org/10.1016/j.aca.2018.07.067